**PRECLINICAL RESEARCH**

Rad GTPase Deletion Attenuates Post-Ischemic Cardiac Dysfunction and Remodeling

Janet R. Manning, PhD,[a,b] Lakshman Chelvarajan, PhD,[c] Bryana M. Levitan, BA,[a,d] Catherine N. Withers, PhD,[b] Prabhakara R. Nagareddy, PhD,[e] Christopher M. Haggerty, PhD,[c,f] Brandon K. Fornwalt, MD, PhD,[c,f] Erhe Gao, MD, PhD,[g] Himi Tripathi, PhD,[c] Ahmed Abdel-Latif, MD, PhD,[c,d] Douglas A. Andres, PhD,[b] Jonathan Satin, PhD[a]

VISUAL ABSTRACT

Loss of Rad Results in Multifaceted Protection Against Post-Ischemic Remodeling
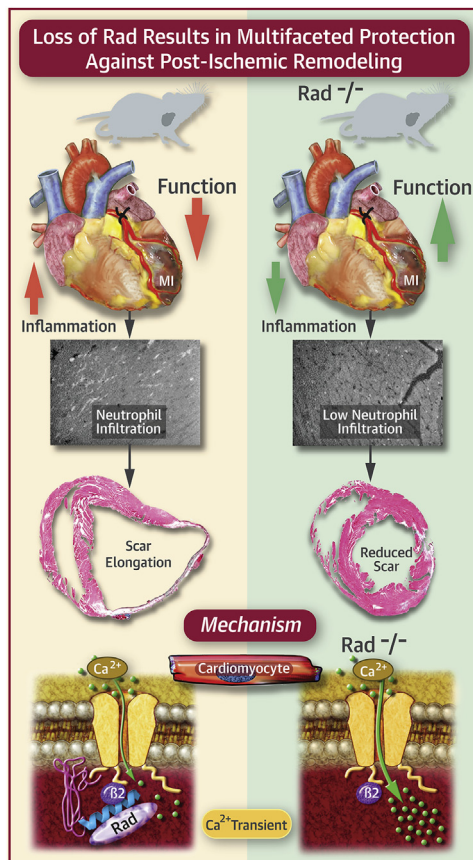
Manning, J.R. et al. J Am Coll Cardiol Basic Trans Science. 2018;3(1):83–96.

HIGHLIGHTS

- Rad-GTPase is an LTCC component that functions to govern calcium current in the myocardium.
- Deletion of Rad increases myocardial contractility secondary to increased trigger calcium entry.
- AMI induces heart failure, including reduced calcium homeostasis, but deletion of Rad prevents AMI myocardial calcium alterations.
- Rad deletion prevents post-MI scar spread by attenuating the inflammatory response.
- Future studies will explore whether Rad deletion is an effective therapeutic direction for providing combined safe, stable inotropic support to the failing heart in concert with protection against inflammatory signaling.

From the [a]Department of Physiology, University of Kentucky, Lexington, Kentucky; [b]Department of Biochemistry, University of Kentucky, Lexington, Kentucky; [c]Saha Cardiovascular Research Center, Department of Medicine, University of Kentucky, Lexington, Kentucky; [d]Gill Heart and Vascular Institute, University of Kentucky, Lexington, Kentucky; [e]Department of Nutrition Sciences, University of Alabama, Birmingham, Alabama; [f]Department of Imaging Science and Innovation, Geisinger, Danville, Pennsylvania; and the [g]Center for Translational Medicine, Temple University School of Medicine, Philadelphia, Pennsylvania.

ABBREVIATIONS
AND ACRONYMS

AMI = acute myocardial infarction

EF = ejection fraction

GTPase = guanosine triphosphatase

HFrEF = heart failure with reduced ejection fraction

LAD = left anterior descending coronary artery

LTCC = L-type calcium channel complex

MI = myocardial infarction

PCR = polymerase chain reaction

RNA = ribonucleic acid

WT = wild-type

SUMMARY

The protein Rad interacts with the L-type calcium channel complex to modulate trigger Ca^{2+} and hence to govern contractility. Reducing Rad levels increases cardiac output. Ablation of Rad also attenuated the inflammatory response following acute myocardial infarction. Future studies to target deletion of Rad in the heart could be conducted to establish a novel treatment paradigm whereby pathologically stressed hearts would be given safe, stable positive inotropic support without arrhythmias and without pathological structural remodeling. Future investigations will also focus on establishing inhibitors of Rad and testing the efficacy of Rad deletion in cardioprotection relative to the time of onset of acute myocardial infarction. (J Am Coll Cardiol Basic Trans Science 2018;3:83–96) © 2018 The Authors. Published by Elsevier on behalf of the American College of Cardiology Foundation. This is an open access article under the CC BY-NC-ND license (http://creativecommons. org/licenses/by-nc-nd/4.0/).

Myocardial infarction (MI) is a leading cause of death in the United States. A cardiac infarct creates a zone containing noncontractile tissue, which compromises the overall mechanical function of the heart. This depresses cardiac output and triggers compensatory hypertrophic growth and remodeling of the myocardium (1,2). Resulting ventricular dilation creates a mechanical disadvantage contributing to a vicious reflexive cycle leading to decompensatory heart failure (heart failure with reduced ejection fraction [HFrEF]). Impaired calcium cycling is a cellular mechanism that contributes to the loss of inotropy in HFrEF. An avenue for investigation therefore becomes the recovery of systolic function via the restoration of healthy calcium cycling. Current treatment of post-MI HFrEF focuses on survival, possibly via relieving cardiac work load using β-adrenergic receptor inhibitors, volume control, reducing cardiac afterload, and preventing further injury from coronary obstruction. However, β-adrenergic receptor inhibition can often have unintended noncardiac side effects and is contraindicated in patients with advanced heart failure. In fact, the reduced contractility of the dilated left ventricle reduces cardiac output to such an extent that pharmacological enhancement of inotropy is required to sustain blood pressure (3,4). In addition, comorbidity often confounds treatment of injury, which can strike patients with HFrEF already reliant on adrenergic stimulation to maintain cardiac output (5), who are at greater risk for death after MI (6). Investigation of strategies that promote cardioprotection from MI without compromising cardiac contractility is therefore of great interest. Proteins that interact with and regulate the L-type calcium channel complex (LTCC) are among this group.

Recent investigations into endogenous regulators of the LTCC have shed light on RGK proteins, a family of small Ras-like guanosine triphosphatases (GTPases) (7–10). RGK proteins are differentially expressed; Rad, an RGK protein expressed in abundance in the heart, has a significant effect on cardiac LTCC current. Rad eliminates current when overexpressed (11); conversely, Rad reduction significantly increases LTCC conductance and twitch calcium (12). We have observed improved contractile function at the cellular and whole-heart levels in uninjured hearts lacking Rad expression (12). This is underscored by the down-regulation of Rad in human heart failure (13), consistent with compensatory regulation to preserve cardiac output. Better systolic function is also associated with improved outcomes after MI (14,15), suggesting that Rad loss may also act as a

compensatory mechanism to recover function in heart failure post-MI.

In addition to compromising function acutely, cardiac ischemia triggers a series of signaling events to communicate with peripheral blood cells and bone marrow that may affect long-term contractile recovery from MI (16). In the first wave of peripheral blood cell response to acute MI (AMI), neutrophils aid in cleanup after tissue damage and the release of proteolytic enzymes. However, this initial injury response may actually confer long-term harm because reduction in the initial recruitment of inflammatory cells reduces infarct size and prevents cardiac remodeling after AMI in mice (16).

In this study, we evaluated the effect of Rad deletion in the response of the myocardium to MI. We found that Rad deletion reduces both mortality and contractile dysfunction after MI. We also found that Rad loss reduces scar development independent of preserving tissue viability, and this finding is accompanied by a reduction in the acute inflammatory response of neutrophil extravasation along with a decrease in inflammatory cytokine signaling.

METHODS

Additional detailed methods are available in the Supplemental Appendix.

MOUSE MODEL. Animals lacking Rad GTPase expression were generated as previously described (17). Cardiac infarct was generated via surgical ligation of the left anterior descending coronary artery (LAD) as previously described (18). All mice were housed and bred on-site, according to the regulations and standards of the University of Kentucky Institutional Animal Care and Use Committee guidelines, which conform to the National Institutes of Health Guide for Care and Use of Laboratory Animals.
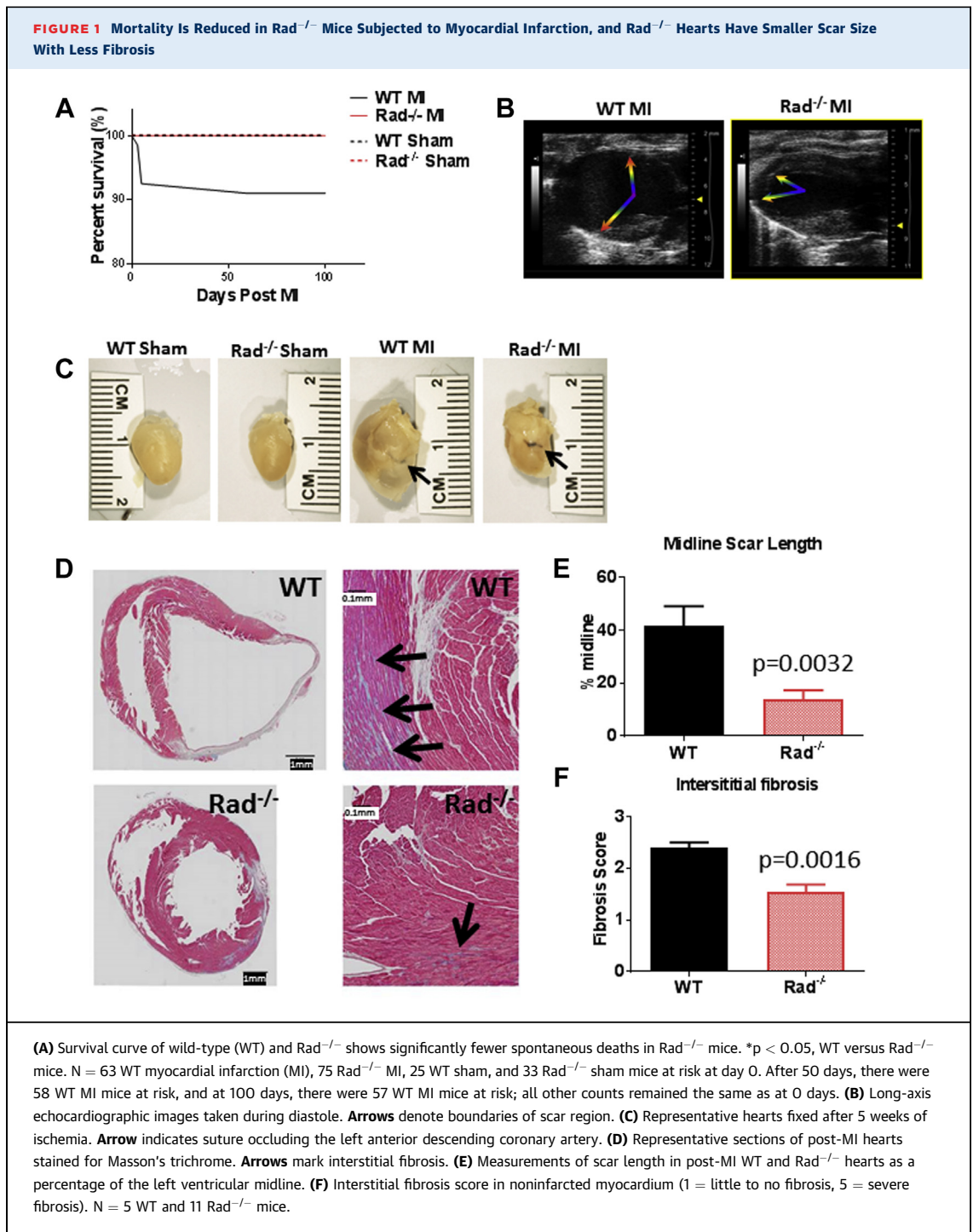
RIBONUCLEIC ACID ISOLATION, MICROARRAY, AND QUANTITATIVE REVERSE-TRANSCRIPTION POLYMERASE CHAIN REACTION. Twenty-four h after MI or sham surgery, tissue from apical regions of the left ventricle was snap frozen in liquid nitrogen. Frozen sections were homogenized in Trizol (Invitrogen, Carlsbad, California). Ribonucleic acid (RNA) was extracted with chloroform followed by isopropanol precipitation and an ethanol wash. The RNA pellet was then treated with DNAse1 (Qiagen, Hilden, Germany) to remove DNA, then precipitated in ammonium acetate and ethanol. After resolubilization, RNA was quantitated and evaluated for quality using the Agilent Bioanalyzer RNA 6000 RNA Nano Kit (Agilent, Santa Clara, California). A Mouse Gene 2.0 ST array was used to probe for gene expression differences between Rad$^{-/-}$ and wild-type (WT) MI hearts for sham and 24 h after LAD ligation. Candidate inflammatory genes identified by this array were validated by quantitative reverse-transcription polymerase chain reaction (PCR) using complementary deoxyribonucleic acid generated with qScript (VWR, Radnor, Pennsylvania) followed by quantitative PCR using TaqMan probes for *Il16*, *Il1b*, *Cxcl1*, *Cxcl2*, *Cxcr2*, and *Tnf* (Thermo Fisher Scientific, Waltham, Massachusetts). Cycle threshold (CT) values were compared to determine statistical significance between groups.

STATISTICAL ANALYSIS. All analyses were done using GraphPad Prism version 7.03 (GraphPad Software, La Jolla, California). Survival curves were compared using a Gehan-Breslow-Wilcoxon test for difference. For simple comparisons between groups, a Student *t* test (for large groups with a Gaussian distribution) or Mann-Whitney *U* test (for small groups) was performed. One-way analysis of variance (for large groups with a Gaussian distribution) or a Kruskal-Wallis test (for small groups) was used to determine statistically significant differences between sham and MI WT and Rad$^{-/-}$ groups for single endpoints, followed by the post hoc Holm-Sidak test (analysis of variance) or Dunn's multiple comparison's test (Kruskal-Wallis test) for individual comparisons. For longitudinal studies examining multiple time points (i.e., all echocardiography time courses, blood pressure data), a repeated-measures 2-way analysis of variance was used. A p value of <0.05 was considered to indicate statistical significance. All values are presented as the mean ± SEM.

RESULTS

RAD DELETION PROTECTS AGAINST AMI-INDUCED MORTALITY. In WT mice, mortality was observed 2 to 5 days after LAD ligation (Figure 1). Deceased mice exhibited blood-filled thoracic cavities consistent with ventricle rupture. No mortality was observed in Rad$^{-/-}$ mice that were ligated at the same time as the WT cohorts, suggesting that Rad loss is protective against ischemia-induced mortality (Figure 1A) (n = 9 WT and 11 Rad$^{-/-}$ mice). Longitudinal-axis echocardiography suggested that Rad$^{-/-}$ had attenuated scar spread at 4 weeks after LAD ligation (Figure 1B). To quantify scar spread 4 to 5 weeks after LAD ligation, hearts were excised from surviving mice, sectioned, and stained with Masson's trichrome. WT and Rad$^{-/-}$ mice showed interstitial collagen deposition as previously described (17), but the extent of scarring was substantially larger in the WT ventricles compared with Rad$^{-/-}$ (Figures 1C to 1E). Furthermore,

FIGURE 1 Mortality Is Reduced in Rad$^{-/-}$ Mice Subjected to Myocardial Infarction, and Rad$^{-/-}$ Hearts Have Smaller Scar Size With Less Fibrosis

(A) Survival curve of wild-type (WT) and Rad$^{-/-}$ shows significantly fewer spontaneous deaths in Rad$^{-/-}$ mice. *p < 0.05, WT versus Rad$^{-/-}$ mice. N = 63 WT myocardial infarction (MI), 75 Rad$^{-/-}$ MI, 25 WT sham, and 33 Rad$^{-/-}$ sham mice at risk at day 0. After 50 days, there were 58 WT MI mice at risk, and at 100 days, there were 57 WT MI mice at risk; all other counts remained the same as at 0 days. **(B)** Long-axis echocardiographic images taken during diastole. **Arrows** denote boundaries of scar region. **(C)** Representative hearts fixed after 5 weeks of ischemia. **Arrow** indicates suture occluding the left anterior descending coronary artery. **(D)** Representative sections of post-MI hearts stained for Masson's trichrome. **Arrows** mark interstitial fibrosis. **(E)** Measurements of scar length in post-MI WT and Rad$^{-/-}$ hearts as a percentage of the left ventricular midline. **(F)** Interstitial fibrosis score in noninfarcted myocardium (1 = little to no fibrosis, 5 = severe fibrosis). N = 5 WT and 11 Rad$^{-/-}$ mice.

noninfarcted regions of the heart were found to contain a greater amount of interstitial fibrosis in WT compared with Rad$^{-/-}$ mice (**Figure 1F**).

POST-ISCHEMIC CARDIAC FUNCTION IS PRESERVED IN RAD$^{-/-}$ MICE. Given the significant difference in mortality and remodeling observed between WT and

Rad$^{-/-}$ mice, we used echocardiography to measure changes in function after LAD ligation. Parallel loss of function occurred in WT and Rad$^{-/-}$ hearts after surgery. Elevated contractility in Rad$^{-/-}$ mice in healthy hearts (prior to LAD ligation) was maintained 24 h after LAD ligation (**Table 1, Figures 2A to 2C**). Ejection fraction values (**Figure 2B**) and fractional

TABLE 1 Hemodynamics Summary

	Heart Rate (beats/min)	Stroke Volume (μl)	Cardiac Output (ml/min)	Ejection Fraction (%)	Fractional Shortening (%)	LVIDd (mm)	LVIDs (mm)
Baseline							
WT	458 ± 8	42 ± 1	20 ± 1	69 ± 1	39 ± 1	3.65 ± 0.05	2.43 ± 0.05
Rad$^{-/-}$	490 ± 7†	41 ± 1	20 ± 1	77 ± 1†	45 ± 1†	3.50 ± 0.04	1.96 ± 0.03
1-day sham							
WT	463 ± 9	29 ± 2	14 ± 1	43 ± 4	22 ± 2	3.80 ± 0.16	2.93 ± 0.13
Rad$^{-/-}$	521 ± 11†	31 ± 2	16 ± 1	64 ± 2†	35 ± 1†	3.42 ± 0.06†	2.27 ± 0.07
1-day MI							
WT	540 ± 13*	18 ± 2*	10 ± 1*	24 ± 2*	11 ± 1*	4.06 ± 0.16	3.69 ± 0.09
Rad$^{-/-}$	501 ± 10	31 ± 3†	16 ± 1†	48 ± 3*†	24 ± 2*†	3.88 ± 0.14*	2.94 ± 0.13*†

Values are mean ± SD. *Significantly different vs. sham at 1 day post-MI. †Significantly different vs. WT at 1 day post-MI.

LVIDd = left ventricular internal dimension in diastole; LVIDs = left ventricular internal dimension in systole; MI = myocardial infarction; WT = wild-type.

shortening values (**Figure 2C**) were higher in Rad$^{-/-}$ compared to WT mice at any given time point. Furthermore, improved outcomes were maintained through 28 days post-surgery (**Figures 2A to 2C**).

We next measured chamber and wall dimensions. Enhanced function in Rad$^{-/-}$ mice was accompanied by a significant difference in the degree of progressive left ventricular chamber dilation and reduced wall thinning. WT hearts demonstrated progressive dilation of the left ventricular diameter at both diastole (**Figure 2D**) and systole (**Figure 2E**); however, no significant dilation was observed in the Rad$^{-/-}$ mice at comparable time points. Similarly, the posterior wall of the ventricle was significantly thicker in the Rad$^{-/-}$ compared with WT mice at 28 days (**Figure 2F**). Anterior wall thickness did not reach significance, but there was a trend toward greater wall thickness in Rad$^{-/-}$ mice (**Figure 2G**). Taken together, these data show that Rad contributes to post-MI structural heart remodeling.

Remodeling in the heart after MI is associated with increased sympathetic stimulation precipitated by a reduction in stroke volume and subsequent decrease in blood pressure. We therefore used echocardiography and blood pressure telemetry to determine whether Rad$^{-/-}$ mice exhibited this initial loss of cardiac output. Cardiac output and stroke volume were not significantly different between WT and Rad$^{-/-}$ mice prior to surgery (**Table 1**). However, WT mice exhibited an initial transient decrease in stroke volume and cardiac output at 24 h post-surgery, while cardiac output and stroke volume in Rad$^{-/-}$ mice were preserved (**Table 1**). In addition, systolic (**Figures 3A and 3B**), diastolic (**Figures 3C and 3D**), and mean arterial blood pressure (**Figures 3E and 3F**) in WT mice dropped significantly after LAD ligation. Conversely, Rad$^{-/-}$ cohorts maintained blood pressures unchanged from baseline levels and significantly higher than WT mice at the same time points.

CALCIUM HANDLING POST-MI IS PRESERVED IN RAD$^{-/-}$ MICE. An important determinant of post-ischemic loss of function in the heart is progressive cellular remodeling resulting in impaired calcium homeostasis. To test whether calcium cycling was preserved in Rad$^{-/-}$ mice, we isolated ventricular myocytes from adult hearts after LAD ligation and measured parameters of stimulated calcium release. We compared WT and Rad$^{-/-}$ cellular Ca^{2+} transients from hearts after 8 weeks of MI (**Figure 4A**). Transient amplitude in the Rad$^{-/-}$ MI group was significantly higher than that of the WT MI counterparts (**Figure 4B**). Similarly, sarcomere shortening was reduced in WT MI but preserved in Rad$^{-/-}$ MI (**Figure 4C**). In addition, the decay constant (tau) of the WT MI group was significantly higher than the sham, suggesting impaired calcium reuptake (**Figure 4D**); in contrast, the calcium reuptake kinetics remained unchanged in the Rad$^{-/-}$ MI versus sham groups (**Figure 4D**). These results suggest that Rad deletion prevents functional post-MI remodeling of calcium handling at the level of the cardiomyocyte.

NO DIFFERENCE WAS OBSERVED IN SUSCEPTIBILITY TO ISCHEMIC TISSUE DEATH OR PERFUSION BETWEEN WT AND RAD$^{-/-}$ MICE. The significant difference observed in infarct scar size between WT and Rad$^{-/-}$ mice suggested the hypothesis that Rad loss induces resistance to ischemia-induced cell death in the border zone of the infarcted heart. Several stimuli have been associated with a preconditioning-like resistance to ischemic tissue death (19–21). We sought to determine whether Rad loss produces a similar effect. Isolated hearts were subjected to

FIGURE 2 Post-Ischemic Loss of Function Is Attenuated in Rad$^{-/-}$ Mice

(A) Representative M-mode echocardiographic tracings of wild-type (WT) and Rad$^{-/-}$ mice 4 weeks after myocardial infarction (MI). **(B,C)** Ejection fraction and fractional shortening for sham and MI (**circles and squares**, respectively) WT (**closed**) and Rad$^{-/-}$ (**open**) mice. **(D,E)** Left ventricular interior dimension values for WT (**closed**) and Rad$^{-/-}$ (**open**) at diastole (LVIDd; **D**) and systole (LVIDs; **E**). **(F)** Left ventricular posterior wall thickness at diastole (LVPWd). **(G)** Left ventricular anterior wall thickness at diastole (LVAWd). N = 19 MI and 28 sham Rad$^{-/-}$ and 30 MI and 38 sham WT mice per group. *p < 0.05, **p < 0.01, ***p < 0.001, and ****p < 0.0001 versus WT MI.

FIGURE 3 Blood Pressure Is Maintained After Left Anterior Descending Coronary Artery Ligation in Rad$^{-/-}$ Mice
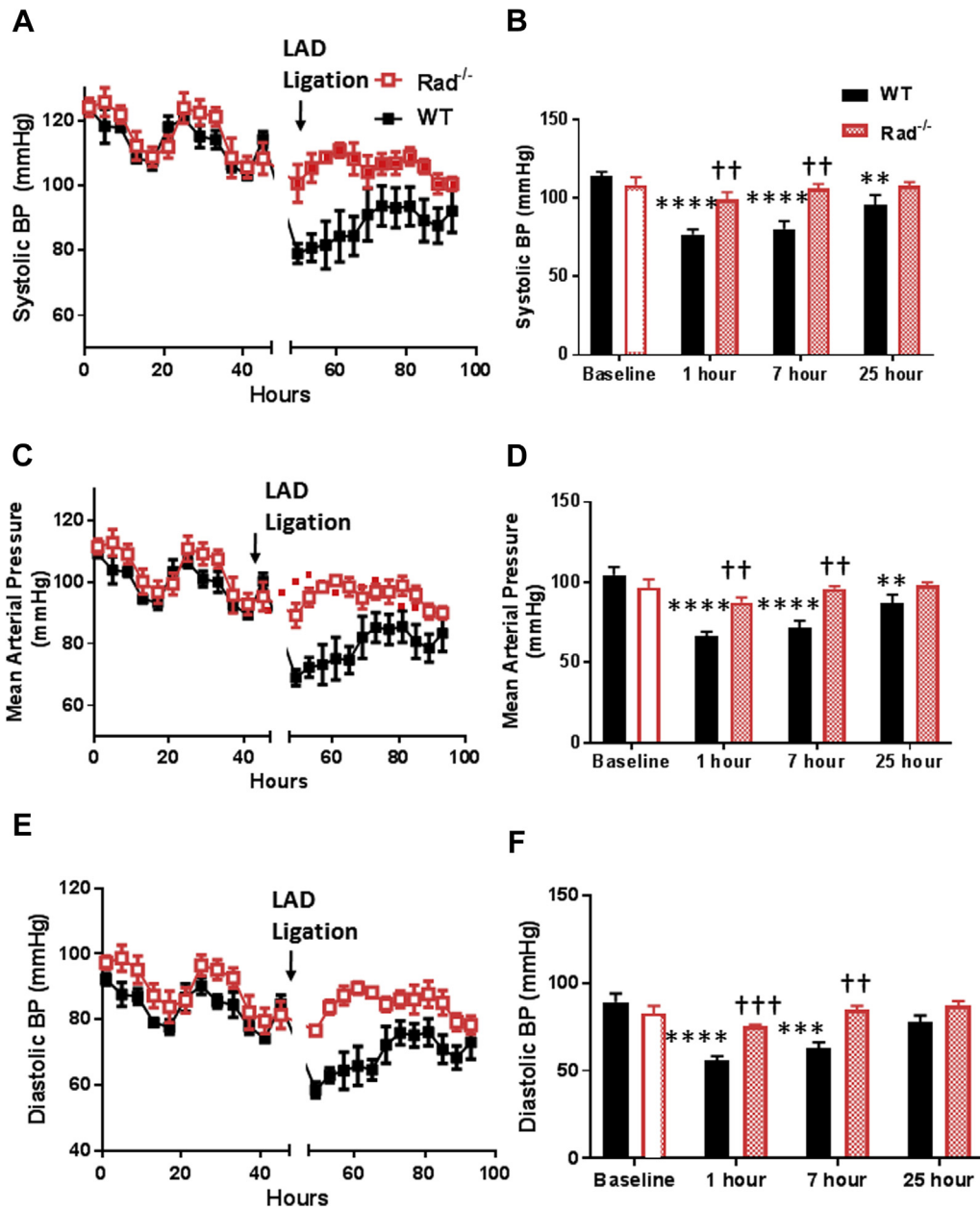
(A,C,E) Longitudinal measurements of systolic (A), mean arterial (C), and diastolic (E) blood pressure (BP) in wild-type (WT) and Rad$^{-/-}$ mice before and after left anterior descending coronary artery (LAD) ligation. (B,D,F) Average measurements of systolic (B), mean arterial (D), and diastolic (F) pressure at baseline prior to surgery, and at single time points of 1, 7, and 25 h after LAD ligation. N = 3 mice per genotype. **p < 0.01, ***p < 0.001, and ****p < 0.0001 versus baseline; ††p < 0.01 and †††p < 0.01 versus WT at same time point.

15 min of global no-flow ischemia, after which viable tissue was immediately stained with triphenyltetrazolium chloride (**Figure 5A**). No difference in infarct was observed between WT and Rad$^{-/-}$ mice (**Figure 5B**), suggesting that Rad loss does not alter death signaling or initial tissue death but rather affects the longer term response of the heart to ischemic damage. We confirmed this finding in vivo using MI induced by LAD ligation, followed by Evans blue/triphenyltetrazolium chloride staining and

FIGURE 4 Calcium Homeostasis Resists Pathological Remodeling in Ventricular Myocytes From Rad$^{-/-}$ After Myocardial Infarction
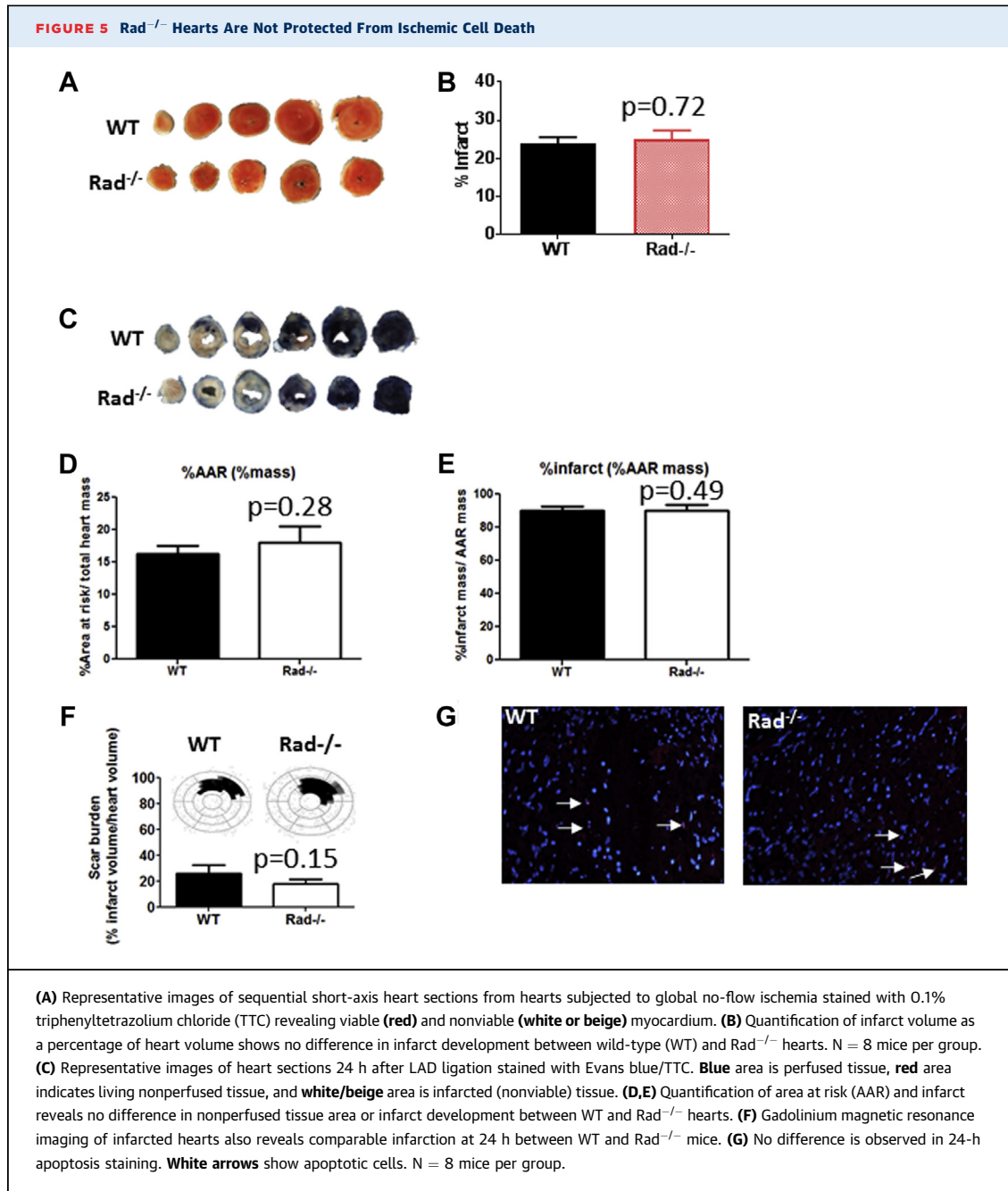

(A) Representative whole-cell Fura-2 recordings for wild-type (WT) and Rad$^{-/-}$ myocytes isolated after sham or 14 weeks after left anterior descending coronary artery ligation. **(B)** Twitch calcium was significantly lowered in WT cells, as expected, but no change was observed in Rad$^{-/-}$ cells. **(C)** Fractional shortening was depressed in WT mice after myocardial infarction (MI) but not in Rad$^{-/-}$ mice. **(D)** Decay constant (tau) is slowed in WT mice by MI but preserved in Rad$^{-/-}$ mice. Data represent the averaged values for each mouse taken as the unit of analysis. N = 16 to 35 cells, n = 9 to 18 mice. *p < 0.05 versus WT sham; †p < 0.01 versus WT MI.

gadolinium magnetic resonance imaging 24 h after surgery (**Figures 5C to 5F**). No significant difference was observed between Rad$^{-/-}$ and WT nonperfused area at risk by Evans blue staining (**Figures 5C and 5D**) or infarct development by triphenyltetrazolium chloride staining (**Figure 5E**). Furthermore, magnetic resonance imaging analysis confirmed that no difference was observed in infarct volume 24 h after MI (**Figure 5G**). We also found no difference in 24-h apoptosis in myocardial sections (**Figure 5H**).

RAD$^{-/-}$ MICE EXHIBIT REDUCED INFLAMMATION AFTER MI.

Post-MI cardiac remodeling occurs stepwise with an initial acute inflammatory response, followed by tissue granulation and then scar formation and spread. Neutrophils are the first immune cell type to infiltrate the heart following MI (22,23), and reduced neutrophil extravasation into myocardial interstitium is linked to protection against MI mortality and scar spread (24,25). Therefore, we next evaluated neutrophil infiltration as an early indicator of the post-ischemic inflammatory response. Histological sections from hearts 24 h post-MI were stained for Ly6G neutrophils and Ly 6C monocytes with the marker GR-1 (**Figure 6A**), and cell density was measured. We found significantly lower neutrophil density in Rad$^{-/-}$ hearts compared with WT hearts (**Figure 6B**). We confirmed the reduction in cardiac neutrophil density using fluorescence-activated cell sorting and counting (**Figure 6C**).

We next examined whether this reduced neutrophil density was associated with generalized

FIGURE 5 Rad$^{-/-}$ Hearts Are Not Protected From Ischemic Cell Death

(A) Representative images of sequential short-axis heart sections from hearts subjected to global no-flow ischemia stained with 0.1% triphenyltetrazolium chloride (TTC) revealing viable **(red)** and nonviable **(white or beige)** myocardium. **(B)** Quantification of infarct volume as a percentage of heart volume shows no difference in infarct development between wild-type (WT) and Rad$^{-/-}$ hearts. N = 8 mice per group. **(C)** Representative images of heart sections 24 h after LAD ligation stained with Evans blue/TTC. **Blue** area is perfused tissue, **red** area indicates living nonperfused tissue, and **white/beige** area is infarcted (nonviable) tissue. **(D,E)** Quantification of area at risk (AAR) and infarct reveals no difference in nonperfused tissue area or infarct development between WT and Rad$^{-/-}$ hearts. **(F)** Gadolinium magnetic resonance imaging of infarcted hearts also reveals comparable infarction at 24 h between WT and Rad$^{-/-}$ mice. **(G)** No difference is observed in 24-h apoptosis staining. **White arrows** show apoptotic cells. N = 8 mice per group.

differences between WT and Rad$^{-/-}$ mice for gene expression induced by MI. We used a Mouse Gene 2.0 ST microarray to identify candidate genes that were up- or down-regulated in Rad$^{-/-}$ ventricular tissue 24 h after MI compared with WT tissue. A plot of all gene changes illustrates a global differential impact of MI on WT versus Rad$^{-/-}$ mice (**Figure 7**). The overall pattern of gene expression changes 24 h after MI suggested that Rad deletion led to a smaller repertoire of gene changes, including a reduced genes and pathways involved in inflammatory response and chemotaxis (data not shown). Proinflammatory cytokines such as interleukin-6, interleukin-1β, and tumor necrosis factor-α are not constitutively expressed in healthy heart but are increased as part of the innate stress response within 24 h post-MI (26). In the microarray, interleukin-6, interleukin-1β, Cxcl1, and Cxcr2 showed comparable, relatively low levels in healthy heart, and MI induced greater changes in WT than Rad$^{-/-}$ mice (**Figure 7**, data not shown). To validate and quantify these changes, we performed quantitative reverse-transcription PCR of selected

FIGURE 6 Neutrophil Counts Are Reduced in Rad$^{-/-}$ Myocardium Compared With Wild-Type After 24 h Myocardial Infarction

(A) Representative images of myocardium stained for Gr-1 as an indicator of neutrophils (white cells). **(B)** Quantification of neutrophil density of 10 averaged random micrographs. N = 5 hearts. **(C)** Fluorescence-activated cell sorting and counting of neutrophil marker–tagged cells in digested hearts. N = 3 sham, 4 wild-type (WT) myocardial infarction (MI) and Rad$^{-/-}$ MI hearts. *p < 0.05 versus WT sham group.

inflammation-related genes (**Figures 8A to 8F**). We also observed in the Rad$^{-/-}$ mice significantly higher levels of basal expression of thrombospondin-4, a protein that has previously been identified as a myocyte-generated anti-inflammatory agent (**Figure 8G**), although no further induction was observed in Rad$^{-/-}$ mice after MI (**Figure 8H**).
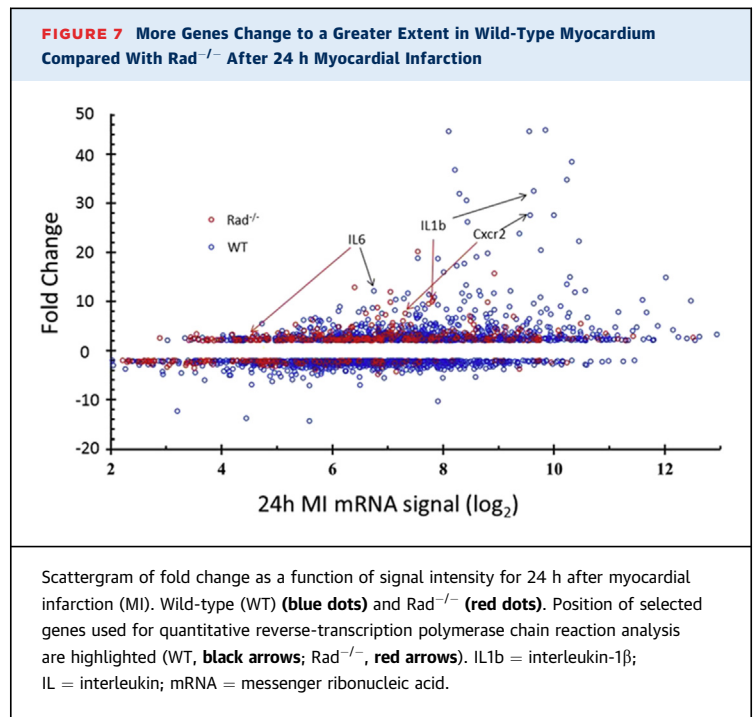
DISCUSSION

The main finding of this study is that deletion of Rad protects the heart against MI. In Rad-knockout mice, scar spread is limited, cardiac function remains higher, and at the level of cardiomyocyte cellular physiology, there is no evidence for pathological post-MI functional remodeling. Rad deletion confers a functional advantage prior to MI that is retained following MI. This study also suggests that Rad may contribute to the inflammatory response following MI. Consequently, Rad$^{-/-}$ mice show cardioprotection secondary to the combination of elevated function prior to MI and attenuated inflammation-induced post-MI cardiac remodeling.
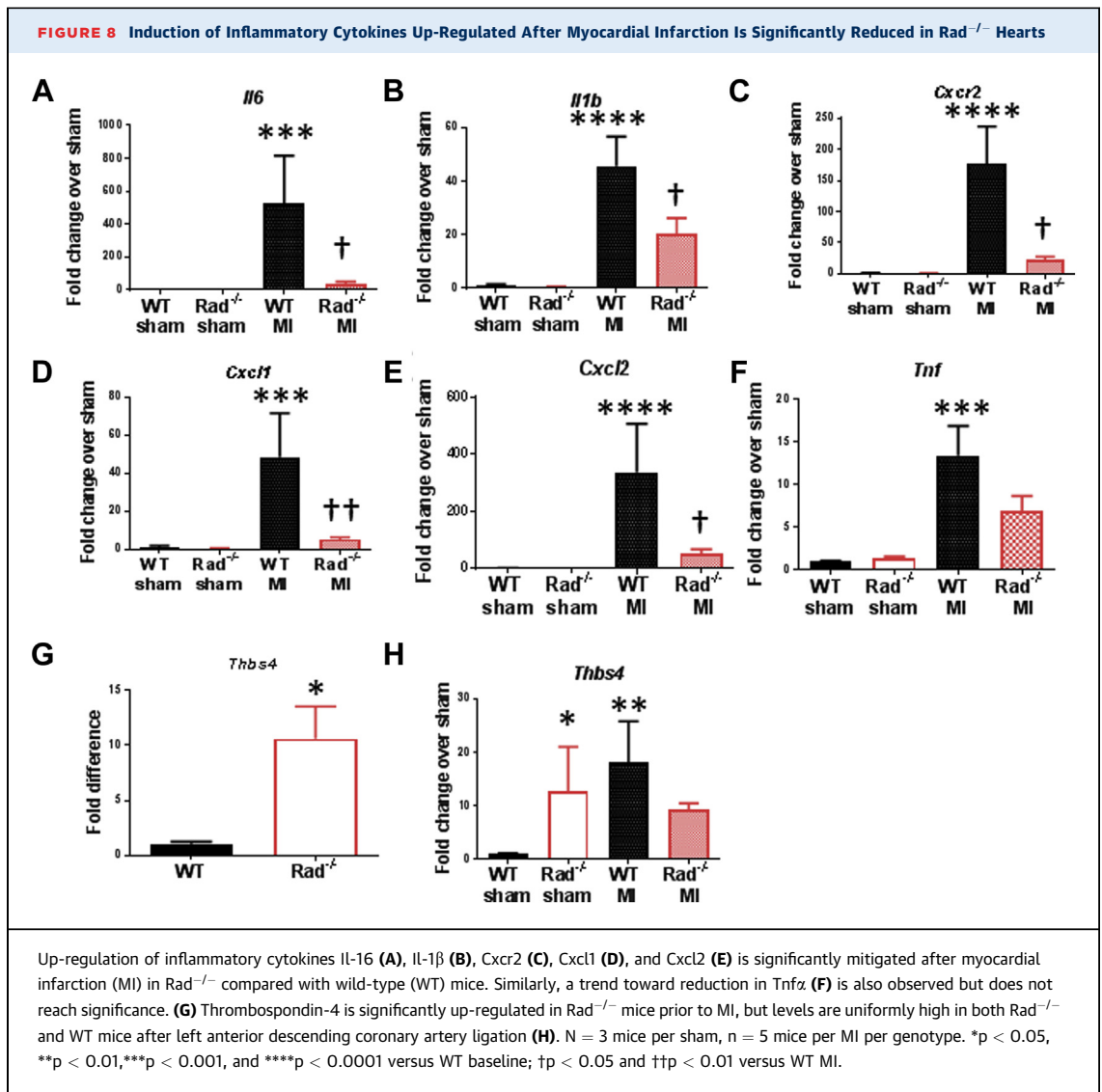
The Rad$^{-/-}$ heart has stable elevated function compared with WT (12,27). This functional gain is preserved 24 h after LAD ligation, although there is a parallel reduction of function in both Rad$^{-/-}$ and MI (**Figure 2**). Nevertheless, function in the Rad$^{-/-}$ mice appears to be sufficiently preserved to avoid the precipitous drop in cardiac output and blood pressure observed in WT mice (**Figure 3**). This acute preservation of function occurs prior to scar spread and myocardial remodeling, suggesting that the improved inotropy associated with Rad deletion (12,27) is maintained after AMI. In WT mice after MI, loss of function results in reflexive, tonic elevation of sympathetic drive that causes pathological cardiomyocyte remodeling. However, the absence of impaired calcium cycling suggests that Rad deletion sufficiently preserves cardiac output to avoid cytological remodeling. This along with earlier findings that Rad$^{-/-}$ is neither arrhythmogenic (12) nor prone to pathological growth (17) draws attention to the new paradigm that distinct regulation of LTCC can be beneficial by improving Ca^{2+} homeostasis (28). In sharp contrast, elevating LTCC via Ca$_V$β2 overexpression enhanced cardiomyocyte trigger Ca^{2+} but led to reduced heart function secondary to cardiomyocyte death (29).

An early study of the Rad$^{-/-}$ mouse showed increased hypertrophy (13); however, it is important to note that this early work performed no functional evaluations. We have now documented stable, chronic positive inotropic function that phenocopies β-adrenergic receptor stimulation in Rad-deficient mice into aging (17,27). Our studies suggest the importance of reevaluating whether Rad-increased Ca^{2+} homeostasis, along with modest cardiac hypertrophy, can form a basis for future safe, stable positive inotropic therapeutic directions.

The loss of Rad may protect the heart from MI in part by blocking the pathological progression of inflammation that follows the initial ischemic insult. The onset of MI is typically followed by a rapid influx of neutrophils, peaking around 24 h after MI (30). Neutrophils then undergo apoptosis, releasing cytokines and chemokines that trigger the infiltration of monocytes and macrophages several days after the beginning of ischemia that clear the dying neutrophils and release cytokines that promote fibrosis and scar formation (24). The impact of this process on healing and outcomes of the heart is complex; although blocking late monocyte infiltration has been shown to be injurious (31), previous experiments have also suggested that blocking neutrophil extravasation is protective against early cardiac rupture and

FIGURE 7 More Genes Change to a Greater Extent in Wild-Type Myocardium Compared With Rad$^{-/-}$ After 24 h Myocardial Infarction

Scattergram of fold change as a function of signal intensity for 24 h after myocardial infarction (MI). Wild-type (WT) **(blue dots)** and Rad$^{-/-}$ **(red dots)**. Position of selected genes used for quantitative reverse-transcription polymerase chain reaction analysis are highlighted (WT, **black arrows**; Rad$^{-/-}$, **red arrows**). IL1b = interleukin-1β; IL = interleukin; mRNA = messenger ribonucleic acid.

pathological remodeling post-MI (32). We propose that in this global Rad$^{-/-}$ knockout, we observe protection against MI-induced pathological remodeling at 2 levels: we observe both a dampened inflammatory response after LAD ligation leading to reduced remodeling and an earlier preservation at 24 h post-MI of the improved contractility in Rad$^{-/-}$ before the effects of inflammation would be expected to affect function. These 2 effects may also be interconnected, given that an important trigger for neutrophil extravasation and inflammation is the sympathetic nervous system, which is activated in the presence of depressed cardiac output (33). Whether the dampened immune response is due to the preservation of sufficient cardiac output to circumvent adrenergic-driven induction and mobilization of neutrophils or whether the global loss of Rad directly affects the maturation and release of neutrophils from bone marrow or spleen remains to be determined. We designed the microarray study to enable discovery of putative signaling pathways that attenuate scar spread and pathological myocardial remodeling in the Rad$^{-/-}$ mouse. Follow-up quantitative reverse-transcription PCR directed by the combination of pathway enrichment analysis and neutrophil extravasation assays (**Figures 6 to 8**) reinforces the utility of our approach to the microarray study.

FIGURE 8   Induction of Inflammatory Cytokines Up-Regulated After Myocardial Infarction Is Significantly Reduced in Rad$^{-/-}$ Hearts

Up-regulation of inflammatory cytokines Il-16 **(A)**, Il-1β **(B)**, Cxcr2 **(C)**, Cxcl1 **(D)**, and Cxcl2 **(E)** is significantly mitigated after myocardial infarction (MI) in Rad$^{-/-}$ compared with wild-type (WT) mice. Similarly, a trend toward reduction in Tnfα **(F)** is also observed but does not reach significance. **(G)** Thrombospondin-4 is significantly up-regulated in Rad$^{-/-}$ mice prior to MI, but levels are uniformly high in both Rad$^{-/-}$ and WT mice after left anterior descending coronary artery ligation **(H)**. N = 3 mice per sham, n = 5 mice per MI per genotype. *p < 0.05, **p < 0.01,***p < 0.001, and ****p < 0.0001 versus WT baseline; †p < 0.05 and ††p < 0.01 versus WT MI.

The observed decrease in early mortality (2 to 5 days) post-MI due to ventricle rupture in Rad$^{-/-}$ mice is consistent with an attenuated inflammatory response as well. Numerous previous studies have demonstrated a significant role for early inflammatory responses in the incidence of rupture, a catastrophic complication of MI that has been described in both mice and humans (34-37). However, it is important to note that deletion of Rad produces a nonpathological increase cardiac wall thickness with mild interstitial fibrosis (17,27). An interesting question that remains is whether these changes in ventricular morphology might work synergistically with reduced inflammatory responses in the Rad$^{-/-}$ to prevent tearing of the wall.

The Rad$^{-/-}$ phenotype has similarities to a cardiac specific knockout of the transforming growth factor-β receptors (32). The transforming growth factor-β receptor knockout model is similarly protected against acute cardiac rupture-associated mortality and scar elongation in a manner that is associated with decreased neutrophil infiltration of the myocardium at early time points after MI. Given that Rad is produced primarily in the cardiomyocyte and not found in observable levels in cardiac fibroblasts (38), Rad and transforming growth factor-β may similarly act as repressors of thrombospondin-4 transcription in myocytes. We note that unlike transforming growth factor-β, we do not observe a difference in thrombospondin-4 expression after MI, suggesting that the hearts of Rad$^{-/-}$ mice may be primed to reduce the inflammatory response prior to ischemic insult, rather

than up-regulate thrombospondin-4 expression after ischemic insult.

CONCLUSIONS

We show here that loss of Rad results in multifaceted protection against post-ischemic remodeling. First, we observe mitigated indexes of post-ischemic failure in both contractile function and ventricular remodeling, concurrent with a preservation of cellular calcium handling. We also observe decreased scar size without decreased infarct volumes, suggesting a dampening of scar elongation processes. This occurs in conjunction with an attenuated inflammatory response, which is further confirmed by decreased neutrophilia in the heart and reduced expression of inflammatory cytokines.

ADDRESS FOR CORRESPONDENCE: Dr. Jonathan Satin, Department of Physiology, MS-508, University of Kentucky College of Medicine, 800 Rose Street, Lexington, Kentucky 40536-0298. E-mail: jsatin1@uky.edu.

PERSPECTIVES

COMPETENCY IN MEDICAL KNOWLEDGE: AMI causes death and remodeling of heart cells leading to heart failure and arrhythmias. Therapeutic options such as those that target the β-adrenergic signaling axis paradoxically reduce heart function. LTCCs provide trigger Ca^{2+} to transduce electric excitation into contraction. Increased LTCC function is a positive inotrope and contributes to heart growth.

TRANSLATIONAL OUTLOOK: The protein Rad interacts with the LTCC to modulate trigger Ca^{2+} and hence to limit contractility. Future studies to target the deletion of Rad in the heart could be conducted to establish a novel treatment paradigm whereby pathologically stressed hearts would be given safe, stable positive inotropic support without arrhythmias and without pathological structural remodeling. Future investigations will also focus on establishing inhibitors of Rad and on testing the efficacy of Rad deletion in cardioprotection relative to the time of onset of AMI.

REFERENCES

1. Dhalla NS, Rangi S, Babick AP, Zieroth S, Elimban V. Cardiac remodeling and subcellular defects in heart failure due to myocardial infarction and aging. Heart Failure Reviews 2012;17: 671–81.

2. Konstam MA, Kramer DG, Patel AR, Maron MS, Udelson JE. Left ventricular remodeling in heart failure: current concepts in clinical significance and assessment. J Am Coll Cardiol Img 2011;4: 98–108.

3. Zhang X, Szeto C, Gao E, et al. Cardiotoxic and cardioprotective features of chronic beta-adrenergic signaling. Circ Res 2013;112: 498–509.

4. Unverferth D, Magorien R, Lewis R, Leier C. Long-term benefit of dobutamine in patients with congestive cardiomyopathy. Am Heart J 1980;100: 622–30.

5. Frishman WH, Saunders E. β-Adrenergic blockers. J Clin Hypertens 2011;13:649–53.

6. Killip T, Kimball JT. Treatment of myocardial infarction in a coronary care unit. A two year experience with 250 patients. Am J Cardiol 1967; 20:457–64.

7. Finlin BS, Correll RN, Pang C, Crump SM, Satin J, Andres DA. Analysis of the complex between Ca^{2+} channel beta-subunit and the Rem GTPase. J Biol Chem 2006;281:23557–66.

8. Correll RN, Botzet GJ, Satin J, Andres DA, Finlin BS. Analysis of the Rem2-voltage dependent calcium channel beta subunit interaction and Rem2 interaction with phosphorylated phosphatidylinositide lipids. Cell Signal 2008;20: 400–8.

9. Crump SM, Correll RN, Schroder EA, et al. L-type calcium channel alpha-subunit and protein kinase inhibitors modulate Rem-mediated regulation of current. Am J Physiol Heart Circ Physiol 2006;291:H1959–71.

10. Finlin BS, Andres DA. Rem is a new member of the Rad- and Gem/Kir Ras-related GTP-binding protein family repressed by lipopoly-saccharide stimulation. J Biol Chem 1997;272: 21982–8.

11. Finlin BS, Crump SM, Satin J, Andres DA. Regulation of voltage-gated calcium channel activity by the Rem and Rad GTPases. Proc Natl Acad Sci U S A 2003;100:14469–74.

12. Manning JR, Yin G, Kaminski CN, et al. Rad GTPase deletion increases L-type calcium channel current leading to increased cardiac contraction. J Am Heart Assoc 2013;2:e000459.

13. Chang L, Zhang J, Tseng YH, et al. Rad GTPase deficiency leads to cardiac hypertrophy. Circulation 2007;116:2976–83.

14. Becker RC, Burns M, Gore JM, et al. Early assessment and in-hospital management of patients with acute myocardial infarction at increased risk for adverse outcomes: a nationwide perspective of current clinical practice. The National Registry of Myocardial Infarction (NRMI-2) Participants. Am Heart J 1998;135:786–96.

15. Steg PG, Dabbous OH, Feldman LJ, et al. Determinants and prognostic impact of heart failure complicating acute coronary syndromes. Observations from the Global Registry of Acute Coronary Events (GRACE) 2004;109:494–9.

16. Zouggari Y, Ait-Oufella H, Bonnin P, et al. B lymphocytes trigger monocyte mobilization and impair heart function after acute myocardial infarction. Nat Med 2013;19:1273–80.

17. Manning JR, Withers CN, Levitan B, Smith JD, Andres DA, Satin J. Loss of Rad-GTPase produces a novel adaptive cardiac phenotype resistant to systolic decline with aging. Am J Physiol Heart Circ Physiol 2015;309:H1336–45.

18. Gao E, Koch WJ. A novel and efficient model of coronary artery ligation in the mouse. Methods Mol Biol 2013;1037:299–311.

19. Miki T, Cohen MV, Downey JM. Opioid receptor contributes to ischemic preconditioning through protein kinase C activation in rabbits. Mol Cell Biochem 1998;186:3–12.

20. Akita T, Abe T, Kto S, Kodama I, Toyama J. Protective effects of diltiazem and ryanodine against ischemia-reperfusion injury in neonatal rabbit hearts. J Thorac Cardiovasc Surg 1993;106:55–66.

21. Ramesh V, Snehasikta S, Mahesh T, Samson Mathews S, Nilanjana M. Ex vivo and in vivo approaches to study mechanisms of cardioprotection targeting ischemia/reperfusion (I/R) injury: useful techniques for cardiovascular drug discovery. Curr Drug Discov Technol 2008;5:269–78.

22. Yan X, Anzai A, Katsumata Y, et al. Temporal dynamics of cardiac immune cell accumulation following acute myocardial infarction. J Mol Cell Cardiol 2013;62:24–35.

23. Frangogiannis NG. Regulation of the inflammatory response in cardiac repair. Circ Res 2012; 110:159–73.

24. Frodermann V, Nahrendorf M. Neutrophil-macrophage cross-talk in acute myocardial infarction. Eur Heart J 2017;38:198–200.

25. Arruda-Olson AM, Reeder GS, Bell MR, Weston SA, Roger VL. Neutrophilia predicts death and heart failure after myocardial infarction: a community-based study. Circ Cardiovasc Qual Outcomes 2009;2:656–62.

26. Nian M, Lee P, Khaper N, Liu P. Inflammatory cytokines and postmyocardial infarction remodeling. Circ Res 2004;94:1543–53.

27. Levitan BM, Manning JR, Withers CN, et al. Rad-deletion phenocopies tonic sympathetic stimulation of the heart. J Cardiovasc Transl Res 2016;9:432–44.

28. Raake PW, Zhang X, Vinge LE, et al. Cardiac G-protein-coupled receptor kinase 2 ablation induces a novel Ca^{2+} handling phenotype resistant to adverse alterations and remodeling after myocardial infarction. Circulation 2012;125:2108–18.

29. Zhang H, Chen X, Gao E, et al. Increasing cardiac contractility after myocardial infarction exacerbates cardiac injury and pump dysfunction. Circ Res 2010;107:800–9.

30. Jung K, Kim P, Leuschner F, et al. Endoscopic time-lapse imaging of immune cells in infarcted mouse hearts: novelty and significance. Circ Res 2013;112:891–9.

31. Nahrendorf M, Swirski FK, Aikawa E, et al. The healing myocardium sequentially mobilizes two monocyte subsets with divergent and complementary functions. J Exp Med 2007;204:3037–47.

32. Rainer PP, Hao S, Vanhoutte D, et al. Cardiomyocyte-specific transforming growth factor β suppression blocks neutrophil infiltration, augments multiple cytoprotective cascades, and reduces early mortality after myocardial infarction: novelty and significance. Circ Res 2014;114:1246–57.

33. Irwin MR, Cole SW. Reciprocal regulation of the neural and innate immune systems. Nat Rev Immunol 2011;11:625–32.

34. Gao X-M, White DA, Dart AM, Du X-J. Post-infarct cardiac rupture: Recent insights on pathogenesis and therapeutic interventions. Pharmacol Ther 2012;134:156–79.

35. Heymans S, Luttun A, Nuyens D, et al. Inhibition of plasminogen activators or matrix metalloproteinases prevents cardiac rupture but impairs therapeutic angiogenesis and causes cardiac failure. Nat Med 1999;5:1135–42.

36. Pouleur A-C, Barkoudah E, Uno H, et al. Pathogenesis of sudden unexpected death in a clinical trial of patients with myocardial infarction and left ventricular dysfunction, heart failure, or both: clinical perspective. Circulation 2010;122:597–602.

37. Roberts WC, Burks KH, Ko JM, Filardo G, Guileyardo JM. Commonalities of cardiac rupture (left ventricular free wall or ventricular septum or papillary muscle) during acute myocardial infarction secondary to atherosclerotic coronary artery disease. Am J Cardiol 2015;115:125–40.

38. Zhang J, Chang L, Chen C, et al. Rad GTPase inhibits cardiac fibrosis through connective tissue growth factor. Cardiovasc Res 2011;91:90–8.

KEY WORDS calcium channel, cardioprotection, inflammation, myocardial infarction

APPENDIX For supplemental methods, please see the online version of this paper.